

Dielectronic-recombination rate coefficients for ions of the oxygen isoelectronic sequence

L. J. Roszman

Atomic and Plasma Radiation Division, National Bureau of Standards, Gaithersburg, Maryland 20899

(Received 11 September 1986)

The rate coefficients for the dielectronic recombination of Ar^{10+} , Fe^{18+} , Kr^{28+} , and Mo^{34+} of the oxygen isoelectronic sequence are computed in the single-configuration, LS -coupled, frozen-core, corona-model approximation. Analytic interpolation formulas for the dielectronic-recombination rate coefficients of the oxygen isoelectronic sequence are given, and comparisons are made with other calculations.

I. INTRODUCTION

The dielectronic-recombination rate coefficients reported here are an extension to the oxygen isoelectronic sequence of a procedure based upon a detailed atomic physics model and an extensive computational technique^{1,2} previously applied to the neon,³ lithium,⁴ and fluorine² isoelectronic sequences. The detail of this model is sufficient to provide accurate coefficients for the total rate of dielectronic recombination of moderately heavy impurity ions in tenuous plasmas⁵ and, with some slight modification, in dense plasmas.^{6,7} The rate coefficients based upon this model can be used to determine the accuracy of the analytic rate coefficient proposed by Burgess⁸ and modified by Merts, Cowan, and Magee.⁹

The application of the general atomic model to the

specific case of the oxygen isoelectronic sequence and a brief description of the computational techniques are contained in Sec. II. The rate coefficients for the dielectronic recombination of ions in the oxygen isoelectronic sequence obtained by the methods of Sec. II, a comparison with the similar rate coefficients obtained by other methods, and analytic fits and interpolation formulas for the computed rate coefficients are presented in Sec. III.

II. ATOMIC MODEL AND COMPUTATIONAL TECHNIQUES

The rate coefficient for the dielectronic recombination of a moderately heavy impurity ion in a tenuous plasma

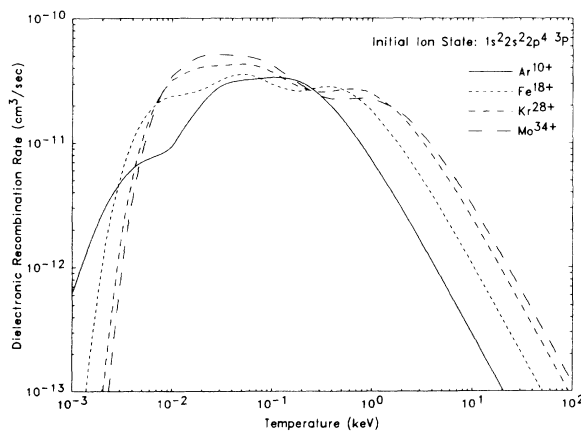


FIG. 1. Detailed calculation of the rate coefficients for the dielectronic recombination of Ar^{10+} , Fe^{18+} , Kr^{28+} , and Mo^{34+} in a low-density plasma when the initial ion is in its ground state $1s^2 2s^2 2p^4 3p$.

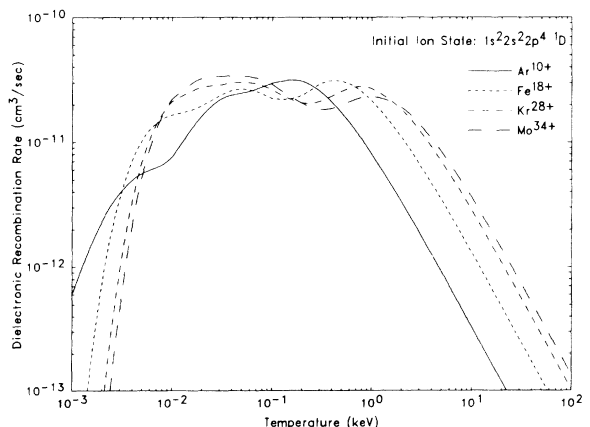


FIG. 2. Detailed calculation of the rate coefficients for the dielectronic recombination of Ar^{10+} , Fe^{18+} , Kr^{28+} , and Mo^{34+} in a low-density plasma when the initial ion is in the state $1s^2 2s^2 2p^4 1D$ of the ground configuration.

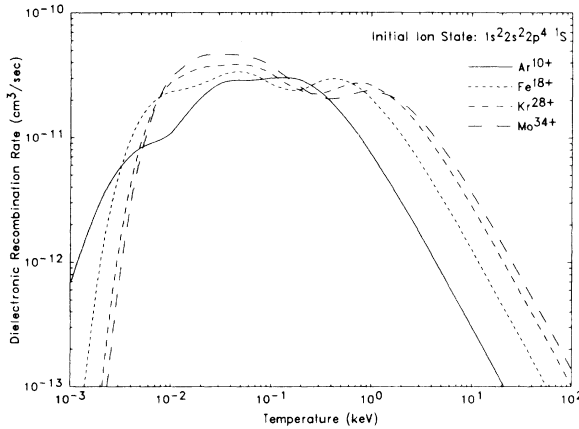


FIG. 3. Detailed calculation of the rate coefficients for the dielectronic recombination of Ar^{10+} , Fe^{18+} , Kr^{28+} , and Mo^{34+} in a low-density plasma when the initial ion is in the state $1s^22s^22p^41S$ of the ground configuration.

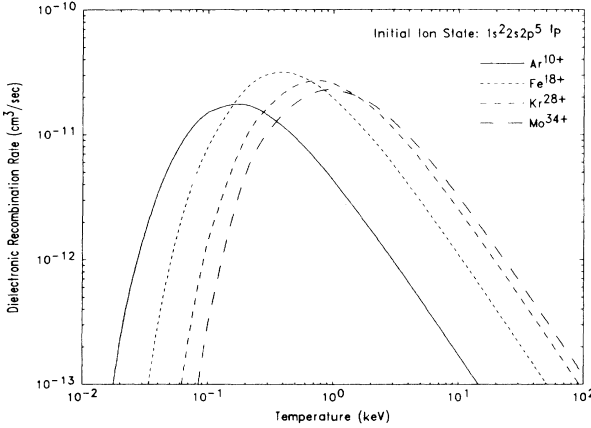


FIG. 4. Detailed calculation of the rate coefficients for the dielectronic recombination of Ar^{10+} , Fe^{18+} , Kr^{28+} , and Mo^{34+} in a low-density plasma when the initial ion is the excited state $1s^22s^22p^51P$.

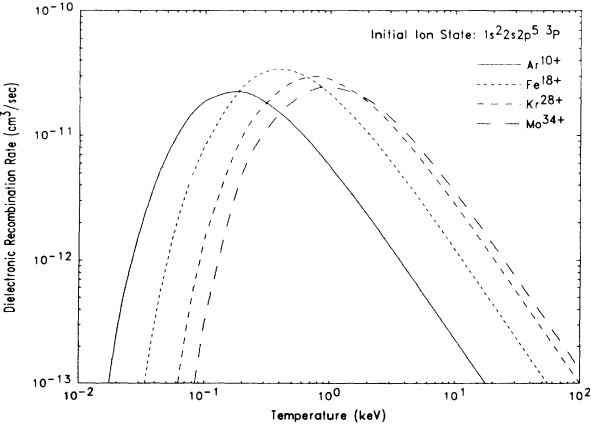


FIG. 5. Detailed calculation of the rate coefficients for the dielectronic recombination of Ar^{10+} , Fe^{18+} , Kr^{28+} , and Mo^{34+} in a low-density plasma when the initial ion state is the excited state $1s^22s^22p^53P$.

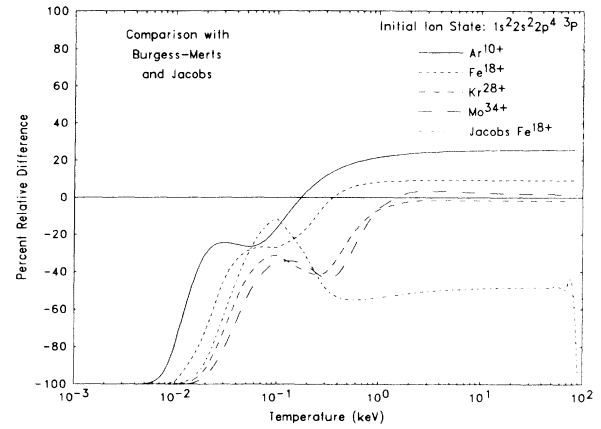


FIG. 6. Percentage differences between the rate coefficients for dielectronic recombination computed from the Burgess-Merts formula for Ar^{10+} , Fe^{18+} , Kr^{28+} and Mo^{34+} , and by Jacobs *et al.*¹⁶ for Fe^{18+} , and those from the detailed calculations when the initial ion state is $1s^22s^22p^43P$.

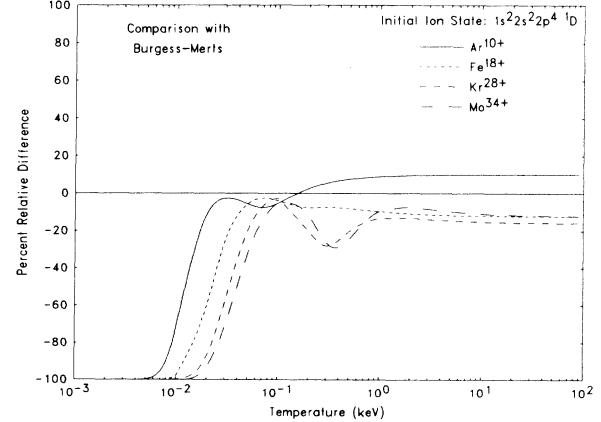


FIG. 7. Percentage differences between the rate coefficients for dielectronic recombination computed from the Burgess-Merts formula and those from the detailed calculations when the initial ion state is $1s^22s^22p^41D$.

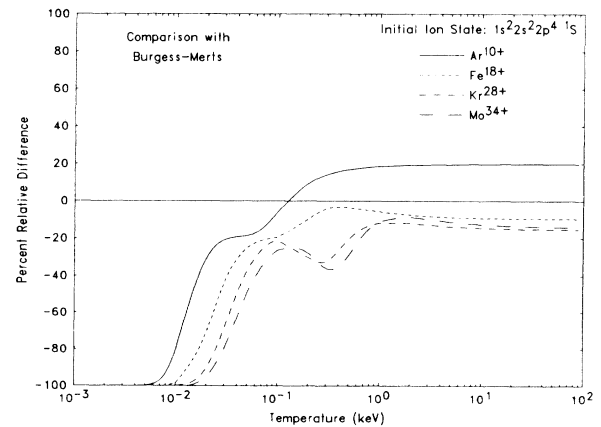


FIG. 8. Percentage differences between the rate coefficients for dielectronic recombination computed from the Burgess-Merts formula and those from the detailed calculations when the initial ion state is $1s^22s^22p^41S$.

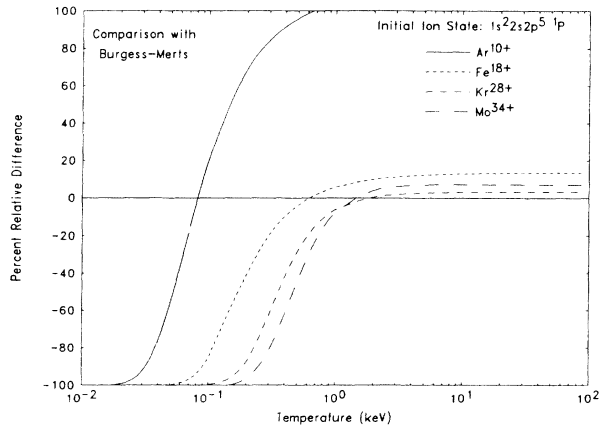


FIG. 9. Percentage differences between the rate coefficients for dielectronic recombination computed from the Burgess-Merts formula and those from the detailed calculations when the initial ion state is $1s^2 2s 2p^5 1P$.

TABLE I. The dielectronic-recombination coefficient for Ar¹⁰⁺ for the initial ion states $1s^2 2s^2 2p^4 3P$, 1D , and 1S and the primary radiative stabilizing transitions $\Delta n \neq 0$.

Temperature (keV)	Dielectronic-recombination rate coefficient for Ar ¹⁰⁺ ($10^{-12} \text{ cm}^3/\text{sec}$)		
	3P	1D	1S
0.02	0.0768	0.0591	0.0538
0.03	0.658	0.509	0.451
0.04	2.00	1.64	1.41
0.05	4.02	3.51	2.96
0.06	6.46	5.95	4.98
0.07	9.02	8.65	7.24
0.08	11.5	11.3	9.53
0.09	13.7	13.9	11.7
0.10	15.6	16.1	13.6
0.20	21.7	24.2	20.9
0.30	19.0	21.7	19.0
0.40	15.7	18.1	15.6
0.50	13.0	15.1	13.4
0.60	10.9	12.7	11.3
0.70	9.30	10.9	9.66
0.80	8.03	9.41	8.36
0.90	7.01	8.23	7.32
1.00	6.18	7.27	6.48
2.00	2.54	3.00	2.68
3.00	1.45	1.72	1.54
4.00	0.966	1.15	1.03
5.00	0.702	0.833	0.746
6.00	0.539	0.641	0.574
7.00	0.431	0.512	0.459
8.00	0.355	0.421	0.378
9.00	0.298	0.355	0.318
10.00	0.256	0.304	0.272
20.00	0.0918	0.109	0.0979
30.00	0.0502	0.0597	0.0535
40.00	0.0327	0.0389	0.0349
50.00	0.0234	0.0279	0.0250
60.00	0.0179	0.0212	0.0190
70.00	0.0142	0.0169	0.0151
80.00	0.0116	0.0138	0.0124
90.00	0.0116	0.0116	0.0104

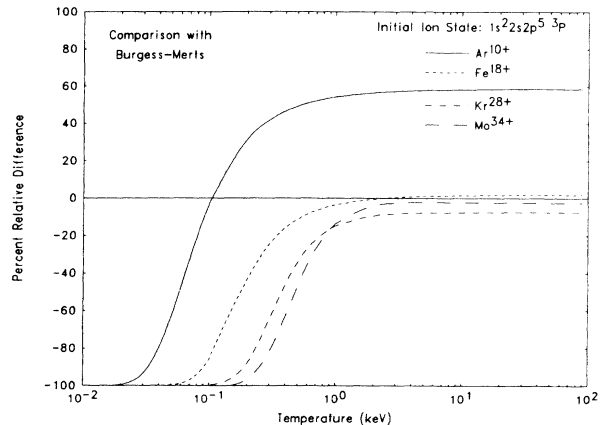


FIG. 10. Percentage differences between the rate coefficients for dielectronic recombination computed from the Burgess-Merts formula and those from the detailed calculations when the initial ion state is $1s^2 2s 2p^5 3P$.

TABLE II. The dielectronic-recombination coefficient for Fe¹⁸⁺ for the initial ion states $1s^2 2s^2 3p^4 3P$, 1D and 1S and the primary radiative stabilizing transitions $\Delta n \neq 0$.

Temperature (keV)	Dielectronic-recombination rate coefficient for Fe ¹⁸⁺ ($10^{-12} \text{ cm}^3/\text{sec}$)		
	3P	1D	1S
0.04	0.0265	0.024	0.0168
0.05	0.0930	0.0815	0.0566
0.06	0.223	0.195	0.135
0.07	0.434	0.385	0.270
0.08	0.744	0.680	0.487
0.09	1.17	1.10	0.810
0.10	1.72	1.67	1.26
0.20	11.0	12.7	10.8
0.30	18.4	22.0	19.6
0.40	21.4	26.1	23.7
0.50	21.9	26.9	24.7
0.60	21.1	26.2	24.3
0.70	19.9	24.8	23.1
0.80	18.6	23.2	21.7
0.90	17.2	21.6	20.3
1.00	16.0	20.0	18.8
2.00	8.15	10.3	9.83
3.00	5.02	6.38	6.09
4.00	3.47	4.42	4.22
5.00	2.58	3.28	3.14
6.00	2.01	2.56	2.45
7.00	1.62	2.07	1.98
8.00	1.35	1.72	1.65
9.00	1.14	1.45	1.40
10.00	0.982	1.25	1.20
20.00	0.360	0.460	0.442
30.00	0.199	0.254	0.244
40.00	0.130	0.166	0.160
50.00	0.0932	0.119	0.114
60.00	0.0711	0.0908	0.0873
70.00	0.0565	0.0722	0.0694
80.00	0.0463	0.059	0.0569
90.00	0.0389	0.0496	0.0477
100.00	0.0332	0.0424	0.0408

$\alpha(i;j;k)$ can be computed from the following expression^{1,10,11}:

$$\alpha(i;j;k) = \frac{4\pi^{3/2}a_0^3}{T^{3/2}g_i} \frac{A_a(j;i\varepsilon_j')Ar(j;k)}{\sum_{i'} A_a(j;i'\varepsilon_{j'}) + \sum_{k'} A_r(j;k')} e^{-\varepsilon_j/T}, \quad (1)$$

where $A_a(j;i\varepsilon_j)$ is the autoionization rate from the state $|j\rangle$ to the continuum state $|i\varepsilon_j'\rangle$ with i denoting the ion core state and ε_j the energy of the continuum orbital in rydberg energy units, $A_r(j;k)$ is the radiative transition rate for the stabilizing transition from the autoionizing state $|j\rangle$ to the bound state $|k\rangle$, the plasma electron temperature T is expressed in atomic units (with the energy in rydbergs), and g_i is the statistical weight of the initial ion state. The quantity a_0 is the Bohr radius. A

frozen-core model of the atomic structure with the single-configuration approximation, Russell-Saunders LS coupling, and the distorted-wave approximation is used to compute the orbital energies, the radiative transition rates, and the autoionization rates.¹⁻⁴ The Hartree-Fock exchange terms which appear in the orbital Schrödinger equations for the bound Rydberg orbitals and for the distorted continuum orbitals are replaced by a variant of the local Cowan HX exchange potential¹² and the local semi-classical exchange potential of Riley and Truhlar,¹³ respectively. The center-of-gravity (spherically averaged) approximation is used in the computation of the orbital energies and wave functions. The complete LS multiplet description is used in the computation of the autoionizing and radiative transition rates, i.e., all possible autoionizing and radiative transition rates are computed for every possible multiplet of a configuration. All dipole-allowed radiative transitions which lead to recombination and all en-

TABLE III. The dielectronic-recombination coefficient for Kr²⁸⁺ for the initial ion states 1s²2s²2p⁴3P, 1D, and 1S and the primary radiative stabilizing transitions $\Delta n \neq 0$.

Temperature (keV)	Dielectronic-recombination rate coefficient for Kr ²⁸⁺ (10 ⁻¹² cm ³ /sec)		
	³ P	¹ D	¹ S
0.06	0.0248	0.0234	0.0217
0.07	0.0823	0.0773	0.0719
0.08	0.198	0.186	0.173
0.09	0.387	0.361	0.337
0.10	0.651	0.608	0.567
0.20	5.65	5.38	4.50
0.30	11.1	11.1	10.4
0.40	15.7	16.3	15.3
0.50	18.8	20.2	19.1
0.60	20.8	22.8	21.6
0.70	21.9	24.2	23.1
0.80	22.2	24.9	23.8
0.90	22.1	25.0	24.0
1.00	21.8	24.7	23.8
2.00	14.9	17.3	16.9
3.00	10.2	12.0	11.7
4.00	7.45	8.76	8.60
5.00	5.72	6.74	6.62
6.00	4.56	5.38	5.29
7.00	3.74	4.42	4.35
8.00	3.14	3.71	3.66
9.00	2.69	3.18	3.13
10.00	2.33	2.76	2.72
20.00	0.885	1.05	1.03
30.00	0.493	0.585	0.577
40.00	0.324	0.385	0.380
50.00	0.234	0.277	0.274
60.00	0.179	0.212	0.209
70.00	0.142	0.169	0.167
80.00	0.118	0.139	0.137
90.00	0.0980	0.116	0.115
100.00	0.0838	0.0995	0.098

TABLE IV. The dielectronic-recombination coefficient for Mo³⁴⁺ for the initial ion states 1s²2s²2p⁴3P, 1D and 1S and the primary radiative stabilizing transitions $\Delta n \neq 0$.

Temperature (keV)	Dielectronic-recombination rate coefficient for Mo ³⁴⁺ (10 ⁻¹² cm ³ /sec)		
	³ P	¹ D	¹ S
0.08	0.0242	0.0234	0.0223
0.09	0.0617	0.598	0.571
0.10	0.129	0.125	0.119
0.20	2.73	2.65	2.55
0.30	6.52	6.45	6.20
0.40	9.91	10.1	9.73
0.50	12.7	13.3	12.9
0.60	15.0	15.9	15.5
0.70	16.5	17.9	17.5
0.80	17.6	19.3	19.0
0.90	18.3	20.3	20.0
1.00	18.7	20.8	20.6
2.00	15.6	17.9	17.9
3.00	11.5	13.4	13.5
4.00	8.76	10.2	10.3
5.00	6.90	8.05	8.14
6.00	5.60	6.54	6.62
7.00	4.65	5.44	5.51
8.00	3.94	4.62	4.68
9.00	3.39	3.98	4.03
10.00	2.96	3.47	3.52
20.00	1.15	1.36	1.38
30.00	0.649	0.764	0.776
40.00	0.429	0.504	0.512
50.00	0.310	0.365	0.370
60.00	0.237	0.279	0.284
70.00	0.189	0.223	0.226
80.00	0.155	0.183	0.186
90.00	0.131	0.154	0.156
100.00	0.112	0.132	0.134

ergetically possible (dipole and nondipole) autoionizing transitions are included.

The Kutta- δ^2 method¹⁴ with the Ridley energy iteration method¹⁵ for the bound orbitals is used to solve the orbital Schrödinger equations. The appropriate Slater integrals are computed using Simpson's "one-third" formula, and the Slater coefficients and angular radiative coefficients are calculated using computer programs which evaluate the appropriate Racah algebra.² The autoionizing and radiative transition rates are computed for a few low-lying states of a Rydberg series and extrapolations to higher states are carried out when necessary. A complete

description of the procedures is contained in previous publications.^{2,4}

The continuum states of the initial ion are based upon the following configurations:

$$1s^2 2s^2 2p^4 \epsilon l \text{ and } 1s^2 2s 2p^5 \epsilon l . \quad (2)$$

The autoionizing states are formed from the following configurations:

$$1s^2 2s^2 2p^3 3nl, 1s^2 2s^2 2p^3 3nl, 1s^2 2s^2 2p^3 3dnl , \quad (3)$$

TABLE V. The dielectronic-recombination coefficient for Ar¹⁰⁺ for the initial ion states 1s²2s²2p⁴³P, ¹D, and ¹S and the primary radiative stabilizing transitions $\Delta n = 0$.

Temperature (keV)	Dielectronic-recombination rate coefficient for Ar ¹⁰⁺ (10 ⁻¹² cm ³ /sec)		
	³ P	¹ D	¹ S
0.001	0.622	0.609	0.682
0.002	2.70	2.34	3.12
0.003	4.76	3.92	5.55
0.004	6.19	4.98	7.25
0.005	7.04	5.61	8.26
0.006	7.54	5.98	8.87
0.007	7.91	6.27	9.31
0.008	8.29	6.60	9.74
0.009	8.80	7.03	10.3
0.010	9.47	7.58	10.9
0.020	20.7	16.4	21.0
0.030	27.6	21.4	26.5
0.040	29.0	22.3	27.2
0.050	27.9	21.3	25.9
0.060	25.9	19.8	23.8
0.070	23.7	18.1	21.7
0.080	21.6	16.4	19.8
0.09	19.7	15.0	18.0
0.10	18.0	13.7	16.4
0.20	8.67	6.54	7.81
0.30	5.23	3.94	4.70
0.40	3.58	2.69	3.21
0.50	2.64	1.99	2.37
0.60	2.05	1.54	1.84
0.70	1.65	1.24	1.48
0.80	1.37	1.03	1.22
0.90	1.16	0.869	1.03
1.00	0.994	0.747	0.888
2.00	0.362	0.272	0.324
3.00	0.199	0.150	0.178
4.00	0.130	0.0978	0.116
5.00	0.0934	0.0701	0.0834
6.00	0.0712	0.0535	0.0636
7.00	0.0566	0.0425	0.0505
8.00	0.0464	0.0348	0.0414
9.00	0.0389	0.0292	0.0347
10.00	0.0332	0.0250	0.0297

TABLE VI. The dielectronic-recombination coefficient for Fe¹⁸⁺ for the initial ion states 1s²2s²2p⁴³P, ¹D, and ¹S and the primary radiative stabilizing transitions $\Delta n = 0$.

Temperature (keV)	Dielectronic-recombination rate coefficient for Fe ¹⁸⁺ (10 ⁻¹² cm ³ /sec)		
	³ P	¹ D	¹ S
0.002	1.05	0.763	1.00
0.003	5.10	3.60	4.92
0.004	10.3	7.20	10.0
0.005	14.9	10.3	14.5
0.006	18.3	12.6	17.8
0.007	20.6	14.2	20.1
0.008	22.2	15.3	21.7
0.009	23.2	16.0	22.7
0.01	23.8	16.5	23.4
0.02	27.0	19.7	27.0
0.03	31.6	23.7	31.1
0.04	34.6	26.1	33.4
0.05	35.4	26.6	33.6
0.06	34.7	26.1	32.6
0.07	33.3	25.0	31.0
0.08	31.5	23.6	29.2
0.09	29.7	22.2	27.3
0.10	27.8	20.7	25.5
0.20	15.2	11.2	13.6
0.30	9.57	7.08	8.57
0.40	6.70	4.95	5.98
0.50	5.01	3.70	4.47
0.60	3.93	2.90	3.50
0.70	3.19	2.35	2.83
0.80	2.65	1.95	2.36
0.90	2.25	1.66	2.00
1.00	1.94	1.43	1.72
2.00	0.718	0.529	0.637
3.00	0.397	0.292	0.352
4.00	0.260	0.191	0.230
5.00	0.187	0.137	0.165
6.00	0.142	0.105	0.126
7.00	0.113	0.0834	0.100
8.00	0.0929	0.0683	0.0822
9.00	0.0779	0.0573	0.0690
10.00	0.0666	0.0490	0.0590
20.00	0.0237	0.0174	0.0209

$$1s^2 2s 2p^5 nl , \quad (4)$$

$$1s^2 2s 2p^4 3snl, 1s^2 2s 2p^4 3pnl, 1s^2 2s 2p^4 3dnl , \quad (5)$$

where n is the principal quantum number of the Rydberg electron. The bound final states are formed from the following configurations:

$$1s^2 2s^2 2p^4 nl \text{ and } 1s^2 2s 2p^5 n'l , \quad (6)$$

where only those states based upon the configuration $1s^2 2s 2p^5 n'l$ which have energies below the first ionization limit are included. The autoionizing states can decay into the following additional continua based upon the excited states of the initial ion when energy constraints allow:

$$1s^2 2s^2 2p^3 3s\epsilon l, 1s^2 2s^2 2p^3 3p\epsilon l, 1s^2 2s^2 2p^3 3d\epsilon l , \quad (7)$$

$$1s^2 2s 2p^4 3s\epsilon l, 1s^2 2s 2p^4 3p\epsilon l, 1s^2 2s 2p^4 3d\epsilon l . \quad (8)$$

TABLE VII. The dielectronic-recombination coefficient for Kr^{28+} for the initial ion states $1s^2 2s 2p^4 {}^3P$, 1D , and 1S and the primary radiative stabilizing transitions $\Delta n = 0$.

Temperature (keV)	Dielectronic-recombination rate coefficient for Kr^{28+} ($10^{-12} \text{ cm}^3/\text{sec}$)		
	3P	1D	1S
0.003	1.42	0.949	1.20
0.004	5.19	3.45	4.43
0.005	10.5	6.98	9.06
0.006	16.2	10.7	14.0
0.007	21.3	14.1	18.5
0.008	25.7	17.0	22.3
0.009	29.2	19.4	25.4
0.01	32.1	21.2	28.0
0.02	40.7	27.5	36.4
0.03	41.7	28.8	37.8
0.04	42.6	29.8	38.5
0.05	42.9	30.2	38.8
0.06	42.4	30.0	37.9
0.07	41.4	29.2	36.7
0.08	39.9	28.2	35.2
0.09	38.2	26.9	33.5
0.10	36.4	25.7	31.8
0.20	22.0	15.3	18.7
0.30	14.5	10.1	12.2
0.40	10.4	7.19	8.71
0.50	7.86	5.45	6.59
0.60	6.22	4.31	5.21
0.70	5.08	3.52	4.25
0.80	4.24	2.94	3.55
0.90	3.62	2.51	3.02
1.00	3.13	2.17	2.61
2.00	1.18	0.813	0.978
3.00	0.653	0.451	0.543
4.00	0.428	0.296	0.356
5.00	0.308	0.213	0.256
6.00	0.235	0.163	0.196
7.00	0.187	0.130	0.156
8.00	0.154	0.106	0.128
9.00	0.129	0.0892	0.107
10.00	0.110	0.0762	0.0916
20.00	0.0392	0.0271	0.0326
30.00	0.0214	0.0148	0.0178

TABLE VIII. The dielectronic-recombination coefficient for Mo^{34+} for the initial ion states $1s^2 2s^2 2p^4 {}^3P$, 1D , and 1S and the primary radiative stabilizing transitions $\Delta n = 0$.

Temperature (keV)	Dielectronic-recombination rate coefficient for Mo^{34+} ($10^{-12} \text{ cm}^3/\text{sec}$)		
	3P	1D	1S
0.003	0.717	0.463	0.624
0.004	3.46	2.23	3.04
0.005	8.29	5.33	7.31
0.006	14.2	9.12	12.5
0.007	20.2	13.0	17.9
0.008	25.7	16.5	22.8
0.009	30.6	19.6	27.1
0.01	34.7	22.3	30.8
0.02	50.1	32.6	45.1
0.03	51.1	33.8	46.5
0.04	50.7	34.1	46.3
0.05	50.0	34.0	45.6
0.06	48.9	33.4	44.4
0.07	47.5	32.6	42.9
0.08	45.8	31.5	41.1
0.09	44.0	30.2	39.2
0.10	42.0	28.9	37.4
0.20	26.1	17.9	22.6
0.30	17.5	12.0	15.0
0.40	12.6	8.64	10.8
0.50	9.63	6.59	8.20
0.60	7.66	5.23	6.50
0.70	6.27	4.28	5.31
0.80	5.25	3.59	4.45
0.90	4.49	3.06	3.79
1.00	3.89	2.65	3.28
2.00	1.47	1.00	1.24
3.00	0.818	0.558	0.689
4.00	0.537	0.366	0.452
5.00	0.387	0.264	0.325
6.00	0.296	0.202	0.249
7.00	0.236	0.160	0.198
8.00	0.193	0.132	0.162
9.00	0.162	0.111	0.136
10.00	0.139	0.0945	0.117
20.00	0.0494	0.0336	0.0415
30.00	0.0269	0.0184	0.0226

The initial ion configuration $1s^2 2s^2 2p^4$ has three LS multiplets, 3P , 1D , and 1S . In the "center-of-gravity" approximation used in this work all these multiplets occur at the same, "ground-state" energy. If the correct term dependences of these multiplets are included, the 3P multiplet is the ground state, and the 1D and 1S multiplets are the first and second excited metastable states of the ground configuration. Since the autoionizing rates do not vary significantly over the energy range of the multiplets, the error introduced into the calculation of the autoionizing rates is negligible. Similarly, the small differences introduced into the energy exponential contained in the expression for the rate coefficient of dielectronic recombination Eq. (1) are negligible. However, in modeling the ionization balance or the kinetics of the plasma there can be ambiguity about the state of the ion before recombination and about

what should be taken as the rate coefficient for dielectronic recombination. The population of the metastable 1D and 1S states of the ground configuration of the oxygen isoelectronic sequence, and, hence, the dielectronic recombination based upon these initial states, depends upon the electron density of the plasma in which the recombination takes place. For the extreme case of a very tenuous plasma, less than 10^8 electrons/cm 3 , in coronal equilibrium, the rate coefficient associated with the ground-state multiplet 3P is the appropriate coefficient to consider. For the other extreme of a dense plasma, 10^{20} or more electrons/cm 3 , the populations of the ground-configuration LS multiplet states are nearly statistical 9:5:1, and one might assume that a summation of the rate coefficients for these states would be appropriate. However, since the rate of dielectronic recombination is signifi-

TABLE IX. The dielectronic-recombination coefficient for Ar^{10+} for the initial ion states $1s^2 2s^2 2p^5 1P$ and 3P .

Temperature (keV)	Dielectronic-recombination rate coefficient for Ar^{10+} (10^{-12} cm 3 /sec)	
	1P	3P
0.02	0.223	0.251
0.03	1.41	1.63
0.04	3.46	4.06
0.05	5.87	6.98
0.06	8.30	9.97
0.07	10.5	12.8
0.08	12.4	15.2
0.09	14.0	17.3
0.10	15.2	18.9
0.20	17.3	22.2
0.30	14.3	18.6
0.40	11.5	15.0
0.50	9.37	12.3
0.60	7.77	10.2
0.70	6.56	8.65
0.80	5.63	7.43
0.90	4.89	6.46
1.00	4.30	5.69
2.00	1.74	2.30
3.00	0.987	1.31
4.00	0.656	8.73
5.00	0.476	0.633
6.00	0.365	0.486
7.00	0.291	0.388
8.00	0.240	0.319
9.00	0.202	0.266
10.00	0.173	0.230
20.00	0.0619	0.0825
30.00	0.0338	0.0451
40.00	0.0220	0.0294
50.00	0.0158	0.0210
60.00	0.0120	0.0160
70.00		0.0127
80.00		0.0104

TABLE X. The dielectronic coefficient for Fe^{18+} for the initial ion states $1s^2 2s^2 2p^5 1P$ and 3P .

Temperature (keV)	Dielectronic-recombination rate coefficient for Fe^{18+} (10^{-12} cm 3 /sec)	
	1P	3P
0.03	0.0410	0.0412
0.04	0.298	0.300
0.05	0.937	0.948
0.06	1.96	1.99
0.07	3.27	3.32
0.08	4.78	4.85
0.09	6.41	6.52
0.10	8.11	8.27
0.20	23.5	24.5
0.30	30.5	32.4
0.40	31.7	34.0
0.50	30.4	32.8
0.60	28.2	30.5
0.70	25.8	28.1
0.80	23.6	25.7
0.90	21.5	23.5
1.00	19.7	21.6
2.00	9.51	10.5
3.00	5.75	6.37
4.00	3.94	4.37
5.00	2.91	3.23
6.00	2.26	2.51
7.00	1.82	2.03
8.00	1.51	1.68
9.00	1.28	1.42
10.00	1.10	1.22
20.00	0.401	0.446
30.00	0.221	0.246
40.00	0.144	0.160
50.00	0.103	0.115
60.00	0.0788	0.0878
70.00	0.0626	0.0698
80.00	0.0513	0.0572
90.00	0.0431	0.0480
100.00	0.0368	0.0410

cantly modified by collisions of the recombining ion with the plasma constituents and, possibly, by containment or electric and magnetic fields produced by the plasma, the "zero-density" rate coefficients described here are not appropriate to the problem. At the plasma densities of fusion devices such as tokamaks, 10^{13} to 10^{14} or 10^{16} electrons/cm³, some intermediate combination of the rate coefficients, requiring modeling of the device, is appropriate. The impact of metastable and of core-excited initial states upon dielectronic recombination will be treated fully elsewhere.

The ions of the oxygen isoelectronic sequence which were considered in these calculations were Ar¹⁰⁺, Fe¹⁸⁺, Kr²⁸⁺, and Mo³⁴⁺. Approximately 400 000 autoionizing rates and 120 000 radiative rates were directly computed for each ion. These rates were extrapolated by the procedures described previously² as needed for the computa-

tion of the total rate coefficients of dielectronic recombination.

III. RESULTS AND COMPARISONS

The dielectronic-recombination rate coefficients for the ions Ar¹⁰⁺, Fe¹⁸⁺, Kr²⁸⁺, and Mo³⁴⁺ are displayed in Figs. 1–5 and tabulated in Tables I–XII. The possible states of the initial ion which were considered are $1s^22s^22p^4{}^3P$, $1s^22s^22p^4{}^1D$, $1s^22s^22p^4{}^1S$, $1s^22s^22p^5{}^1P$, and $1s^22s^22p^5{}^3P$. The rate coefficients displayed in Figs. 1–3, which are associated with the ground configuration $1s^22s^22p^4$ are based upon the summation of those rate coefficients which have stabilizing radiative transitions in which the principal quantum number of the radiating electron changes ($\Delta n \neq 0$) and in which it does not change ($\Delta n = 0$). The rate coefficients of Figs. 4 and 5, which are associated with the core-excited configuration $1s^22s^22p^5$

TABLE XI. The dielectronic-recombination coefficient for Kr²⁸⁺ and for the initial ion states $1s^22s^22p^5{}^1P$ and 3P .

Temperature (keV)	Dielectronic-recombination rate coefficient for Kr ²⁸⁺ (10^{-12} cm ³ /sec)	
	1P	3P
0.05	0.0160	0.0162
0.06	0.0758	0.0769
0.07	0.224	0.229
0.08	0.496	0.507
0.09	0.903	0.925
0.10	1.44	1.48
0.20	9.01	9.32
0.30	14.1	14.6
0.40	16.4	17.0
0.50	17.3	18.0
0.60	17.4	18.1
0.70	17.0	17.7
0.80	16.4	17.0
0.90	15.7	16.3
1.00	14.9	15.5
2.00	8.82	9.18
3.00	5.76	6.00
4.00	4.11	4.28
5.00	3.11	3.24
6.00	2.46	2.56
7.00	2.01	2.09
8.00	1.68	1.75
9.00	1.43	1.49
10.00	1.23	1.29
20.00	0.462	0.483
30.00	0.257	0.268
40.00	0.168	0.176
50.00	0.121	0.127
60.00	0.0926	0.0967
70.00	0.0737	0.0769
80.00	0.0604	0.0631
90.00	0.0507	0.0529
100.00	0.0434	0.0453

TABLE XII. The dielectronic-recombination coefficient for Mo³⁴⁺ and for the initial ion states $1s^22s^22p^5{}^1P$ and 3P .

Temperature (keV)	Dielectronic-recombination rate coefficient for Mo ³⁴⁺ (10^{-12} cm ³ /sec)	
	1P	3P
0.07	0.0216	0.0216
0.08	0.0666	0.0667
0.09	0.158	0.158
0.10	0.310	0.311
0.20	4.93	4.98
0.30	10.5	10.7
0.40	14.8	15.3
0.50	18.0	18.7
0.60	20.3	21.2
0.70	21.7	22.9
0.80	22.6	24.0
0.90	23.0	24.5
1.00	23.1	24.7
2.00	17.8	19.3
3.00	12.9	14.0
4.00	9.65	10.5
5.00	7.54	8.24
6.00	6.08	6.66
7.00	5.04	5.51
8.00	4.26	4.66
9.00	3.66	4.01
10.00	3.19	3.49
20.00	1.23	1.35
30.00	0.692	0.759
40.00	0.456	0.501
50.00	0.329	0.362
60.00	0.252	0.277
70.00	0.201	0.221
80.00	0.165	0.181
90.00	0.139	0.152
100.00	0.119	0.130

have, of course, only $\Delta n \neq 0$ radiative stabilizing transitions. The rate coefficients for the various initial states and the $\Delta n \neq 0$ and $\Delta n = 0$ radiative stabilizing processes are tabulated separately in Tables I–XII.

The plots of Figs. 1–3 for the rate coefficients associated with the ground configuration $1s^2 2s^2 2p^4$ display the separate peaks and shoulders of the $\Delta n \neq 0$ and the $\Delta n = 0$ transitions, and of lowest-lying autoionizing state of the configuration $1s^2 2s 2p^4 nl$ noted in previous works.^{2,4} In general the low-energy shoulder occurs because of the lowest-lying $1s^2 2s 2p^5 nl$ state, the lowest-energy peak is generated by the $\Delta n = 0$ radiative stabilizing transitions, and the highest-energy peak is associated with the $\Delta n \neq 0$ radiative transitions. The definition of the peaks and shoulders for each ion depends upon the extent of the energy range of the autoionizing states associated with the $\Delta n \neq 0$ and with the $\Delta n = 0$ radiative transitions, and upon the relative energy positions of the lowest-lying $1s^2 2s 2p^5 nl$ state and of those states associated with the $\Delta n \neq 0$ radiative transitions.

Comparisons between the total rate coefficients for the dielectronic recombination of Ar^{10+} , Fe^{18+} , Kr^{28+} , and Mo^{34+} computed by the methods described in Sec. II and

those obtained by taking the summation of the Burgess analytic formula⁸ for $\Delta n = 0$ radiative stabilizing transitions and of the variation of the Burgess formula for $\Delta n \neq 0$ radiative stabilizing transitions suggested by Merts, Cowan, and Magee⁹ are displayed in Figs. 6–10. Also, displayed in Fig. 6 is a comparison with the total rate coefficient of dielectronic recombination for Fe^{18+} , when the initial ion is in its ground state $1s^2 2s^2 2s^4 3P$, computed with a different detailed method by Jacobs, Davis, Kepple, and Blaha.^{16,17} The radiative transition rates and excitation energies used in the Burgess-Merts formula were computed using center-of-gravity wave functions obtained from the computer code of Fischer.¹⁸

The extreme difference between the dielectronic-recombination rate coefficient for Fe^{18+} reported here and the similar rate coefficient computed by Jacobs, Davis, Kepple, and Blaha¹⁶ appears to be due to the omission by Jacobs, David, Kepple, and Blaha of all autoionizing and inverse autoionizing transitions not based upon the allowed radiative dipole transitions of the initial (unrecombined) ion,^{2,4} to the neglect of radiative stabilizing transitions into the bound, double-excited (core-excited) states of the $1s^2 2s 2p^5 nl$ configurations which are below the first

TABLE XIII. The coefficients and parameters for the fit of the exponential series $\alpha = T^{-3/2} \sum_i c_i \exp(-\xi_i/T)$ to the directly computed dielectronic-recombination rate coefficients when the initial ion is in one of the states of the ground configuration $1s^2 2s^2 2p^4$, 3P , 1D , or 1S and the radiative transition have principal quantum number change $\Delta n = 0$.

Ion	Ar^{10+}	Fe^{18+}	Kr^{28+}	Mo^{34+}
State: $1s^2 2s^2 2p^4 3P$				
c_1	2.26×10^{-12}	5.19×10^{-11}	1.59×10^{-10}	2.44×10^{-10}
ξ_1	0.400	1.01	1.55	1.80
c_2	1.42×10^{-11}	9.15×10^{-11}	2.85×10^{-10}	4.48×10^{-10}
ξ_2	1.06	2.84	4.27	4.84
c_3	6.44×10^{-10}	1.19×10^{-9}	1.78×10^{-9}	2.10×10^{-9}
ξ_3	4.60	7.20	10.3	11.9
State: $1s^2 2s^2 2p^4 1D$				
c_1	1.69×10^{-12}	3.48×10^{-11}	1.05×10^{-10}	1.57×10^{-10}
ξ_1	0.377	1.00	1.55	1.80
c_2	1.14×10^{-11}	7.43×10^{-11}	2.12×10^{-10}	3.13×10^{-10}
ξ_2	1.06	2.88	4.32	4.8
c_3	4.82×10^{-10}	8.72×10^{-10}	1.22×10^{-9}	1.43×10^{-9}
ξ_3	4.53	7.08	10.1	11.7
State: $1s^2 2s^2 2p^4 1S$				
c_1	3.02×10^{-12}	5.07×10^{-11}	1.40×10^{-10}	2.19×10^{-10}
ξ_1	0.420	1.02	1.56	1.80
c_2	1.72×10^{-11}	1.01×10^{-10}	2.77×10^{-10}	4.25×10^{-10}
ξ_2	1.10	2.89	4.32	4.86
c_3	5.68×10^{-10}	1.03×10^{-9}	1.42×10^{-9}	1.70×10^{-9}
ξ_3	4.49	7.02	9.98	11.5

TABLE XIV. The coefficients and parameters for the fit of the exponential series $\alpha = T^{-3/2} \sum_i c_i \exp(-\xi_i/T)$ to the directly computed dielectronic-recombination rate coefficients when the initial ion is in one of the states of the ground configuration $1s^2 2s^2 2p^4$, 3P , 1D , or 1S and the radiative transitions have principal quantum number change $\Delta n \neq 0$.

Ion	Ar^{10+}	Fe^{18+}	Kr^{28+}	Mo^{34+}
State: $1s^2 2s^2 2p^4 {}^3P$				
c_1	3.31×10^{-10}	3.58×10^{-10}	5.01×10^{-9}	8.93×10^{-9}
ξ_1	11.5	23.4	44.0	128.5
c_2	1.80×10^{-9}	6.40×10^{-9}	9.28×10^{-9}	2.78×10^{-8}
ξ_2	19.0	44.3	75.3	128.5
c_3	3.13×10^{-9}	1.44×10^{-8}	3.93×10^{-8}	3.52×10^{-8}
ξ_3	24.9	60.5	120.4	181.1
State: $1s^2 2s^2 2p^4 {}^1D$				
c_1	2.33×10^{-10}	2.90×10^{-10}	4.28×10^{-9}	8.53×10^{-9}
ξ_1	11.4	23.1	43.4	60.0
c_2	1.93×10^{-9}	8.25×10^{-9}	9.88×10^{-9}	3.19×10^{-8}
ξ_2	19.4	45.7	73.8	128.5
c_3	4.09×10^{-9}	1.84×10^{-8}	4.94×10^{-8}	4.43×10^{-8}
ξ_3	25.2	61.3	129.5	180.6
State: $1s^2 2s^2 2p^4 {}^1S$				
c_1	2.25×10^{-10}	2.03×10^{-10}	3.37×10^{-9}	8.24×10^{-9}
ξ_1	11.5	23.2	42.5	60.1
c_2	1.69×10^{-9}	7.57×10^{-9}	7.79×10^{-9}	3.00×10^{-8}
ξ_2	19.9	47.0	67.4	128.5
c_3	3.69×10^{-9}	1.82×10^{-8}	5.16×10^{-8}	4.78×10^{-8}
ξ_3	25.8	62.7	120.6	180.7

TABLE XV. The coefficients and parameters for the fit of the exponential series $\alpha = T^{-3/2} \sum_i c_i \exp(-\xi_i/T)$ to the directly computed dielectronic-recombination rate coefficients when the initial ion is in one of the states of the ground configuration $1s^2 2s 2p^5$, 3P , or 1P .

Ion	Ar^{10+}	Fe^{18+}	Kr^{28+}	Mo^{34+}
State: $1s^2 2s 2p^5 {}^1P$				
c_1	4.63×10^{-10}	2.36×10^{-9}	7.83×10^{-9}	1.24×10^{-8}
ξ_1	10.4	21.7	41.3	56.1
c_2	1.18×10^{-9}	6.97×10^{-9}	1.78×10^{-8}	3.71×10^{-8}
ξ_2	17.2	39.9	84.7	128.5
c_3	1.90×10^{-9}	1.40×10^{-8}	3.14×10^{-8}	2.68×10^{-8}
ξ_3	23.5	55.4	120.2	179.9
State: $1s^2 2s 2p^5 {}^3P$				
c_1	5.51×10^{-10}	2.45×10^{-9}	8.14×10^{-9}	1.25×10^{-8}
ξ_1	10.5	21.8	41.4	56.2
c_2	1.49×10^{-9}	8.18×10^{-9}	1.96×10^{-8}	4.06×10^{-8}
ξ_2	17.3	40.9	84.5	128.5
c_3	2.68×10^{-9}	1.54×10^{-8}	3.60×10^{-8}	3.06×10^{-8}
ξ_3	24.0	57.0	120.3	180.2

ionization limit, to the use of the extrapolation procedure of the quantum defect theory, and to the particular partial-wave excitation cross sections used in the extrapolation procedure. The first of these approximations is the most significant and introduces most of the difference between these two calculations.^{2,4}

Tables XIII–XV contain the parameters ξ_i and the coefficients c_i obtained from a fit of the sum of three exponentials,^{2,4}

$$\alpha = T^{-3/2} \sum_{i=1}^3 c_i e^{\xi_i/T}, \quad (9)$$

to the rate coefficients of dielectronic recombination for the ions Ar¹⁰⁺, Fe¹⁸⁺, Kr²⁸⁺, and Mo³⁴⁺ computed by the methods described in Sec. II and tabulated in Tables I–XII. Generally, these fits reproduce the directly computed data to 0.1% over the indicated temperature ranges.

Tables XVI–XVIII contain the coefficients which can be used to interpolate the parameters ξ_i and the coefficients c_i for other members of the oxygen isoelectronic sequence. The coefficients of Table XVI are used in the following equations for ξ_i and c_i associated with $\Delta n=0$ radi-

ative stabilizing transitions:

$$\log_{10}(c_i) = \sum_{j=1}^4 a_{ij} z^{j-1}, \quad (10)$$

and

$$\xi_i = z^4 \sum_{j=1}^3 b_{ij} z^{1-j}. \quad (11)$$

Tables XVII and XVIII contain the interpolation coefficients of the following formula which are associated with the radiative transitions $\Delta n \neq 0$ for the various initial states:

$$\log_{10}(c_i) = \sum_{j=1}^4 a_{ij} [\log_{10}(z)]^{j-1}, \quad (12)$$

and

$$\xi_i = z^2 \sum_{j=1}^3 b_{ij} z^{1-j}. \quad (13)$$

A linear least-squares fit to the data of Tables I–XII was used to determine these coefficients.

TABLE XVI. The interpolation coefficients for the oxygen sequence when the initial ion in one of the states $1s^2 2s^2 2p^4 3P$, $1D$, or $1S$ and the radiative transitions are $\Delta n=0$: $\log_{10}(c_i) = \sum_{j=1}^4 a_{ij} z^{j-1}$ and $\xi_i = z^4 \sum_{j=1}^3 b_{ij} z^{1-j}$, where z is the effective charge of the initial ion.

<i>j</i>	1	2	3	4
State: $1s^2 2s^2 2p^4 3P$				
a_{1j}	$-1.57 \times 10^{+1}$	5.86×10^{-1}	-1.99×10^{-2}	2.35×10^{-4}
b_{1j}	3.27×10^{-7}	-1.20×10^{-4}	5.17×10^{-3}	
a_{2j}	$-1.28 \times 10^{+1}$	2.55×10^{-1}	-7.14×10^{-3}	7.62×10^{-5}
b_{2j}	-3.24×10^{-6}	-1.40×10^{-4}	1.23×10^{-2}	
a_{3j}	-9.80	8.11×10^{-2}	-2.21×10^{-3}	2.36×10^{-5}
b_{3j}	9.67×10^{-5}	-5.64×10^{-3}	9.27×10^{-2}	
State: $1s^2 2s^2 2p^4 1D$				
a_{1j}	$-1.57 \times 10^{+1}$	5.58×10^{-1}	-1.88×10^{-2}	2.20×10^{-4}
b_{1j}	-6.63×10^{-7}	-6.83×10^{-5}	4.52×10^{-3}	
a_{2j}	$-1.29 \times 10^{+1}$	2.72×10^{-1}	-7.93×10^{-3}	8.57×10^{-5}
b_{2j}	-3.91×10^{-6}	-1.11×10^{-4}	1.21×10^{-2}	
a_{3j}	-9.99	9.26×10^{-2}	-2.89×10^{-3}	3.41×10^{-5}
b_{3j}	9.52×10^{-5}	-5.55×10^{-3}	9.13×10^{-2}	
State: $1s^2 2s^2 2p^4 1S$				
a_{1j}	$-1.53 \times 10^{+1}$	5.35×10^{-1}	-1.84×10^{-2}	2.21×10^{-4}
b_{1j}	-2.16×10^{-6}	-2.02×10^{-4}	1.32×10^{-2}	
a_{2j}	$-1.27 \times 10^{+1}$	2.62×10^{-1}	-7.79×10^{-3}	8.72×10^{-5}
b_{2j}	-2.16×10^{-6}	-2.02×10^{-4}	1.32×10^{-2}	
a_{3j}	-9.95	9.77×10^{-2}	-3.17×10^{-3}	3.86×10^{-5}
b_{3j}	9.43×10^{-5}	-5.50×10^{-3}	9.05×10^{-2}	

TABLE XVII. The interpolation coefficients for the oxygen sequence when the initial ion in one of the states $1s^22s^22p^4{}^3P$, 1D , or 1S and the radiative transitions are $\Delta n \neq 0$: $\log_{10}(c_i) = \sum_{j=1}^4 a_{ij} z^{j-1}$ and $\xi_i = z^2 \sum_{j=1}^3 b_{ij} z^{1-j}$, where z is the effective charge of the initial ion.

j	1	2	3	4
State: $1s^22s^22p^4{}^3P$				
a_{1j}	$8.85 \times 10^{+1}$	$-2.33 \times 10^{+2}$	$1.80 \times 10^{+2}$	$-4.50 \times 10^{+1}$
b_{1j}	3.34×10^{-2}	5.48×10^{-1}	2.71	
a_{2j}	$-8.40 \times 10^{+1}$	$1.81 \times 10^{+2}$	$-1.44 \times 10^{+2}$	$3.82 \times 10^{+1}$
b_{2j}	7.21×10^{-2}	9.57×10^{-1}	2.24	
a_{3j}	$2.07 \times 10^{+1}$	$-7.72 \times 10^{+1}$	$6.60 \times 10^{+1}$	$-1.80 \times 10^{+1}$
b_{3j}	1.21×10^{-1}	9.61×10^{-1}	3.16	
State: $1s^22s^22p^4{}^1D$				
a_{1j}	$8.14 \times 10^{+1}$	$-2.16 \times 10^{+2}$	$1.66 \times 10^{+2}$	$-4.15 \times 10^{+1}$
b_{1j}	3.43×10^{-2}	5.01×10^{-1}	2.97	
a_{2j}	$-1.02 \times 10^{+2}$	$2.25 \times 10^{+2}$	$-1.79 \times 10^{+2}$	$4.70 \times 10^{+1}$
b_{2j}	6.07×10^{-2}	1.37	-3.12×10^{-1}	
a_{3j}	$2.03 \times 10^{+1}$	$-7.57 \times 10^{+1}$	$6.47 \times 10^{+1}$	$-1.77 \times 10^{+1}$
b_{3j}	1.15×10^{-1}	1.22	1.55	
State: $1s^22s^22p^4{}^1S$				
a_{1j}	$8.05 \times 10^{+1}$	$-2.11 \times 10^{+2}$	$1.61 \times 10^{+2}$	$-3.94 \times 10^{+1}$
b_{1j}	3.35×10^{-2}	5.05×10^{-1}	3.07	
a_{2j}	$-1.22 \times 10^{+2}$	$2.74 \times 10^{+2}$	$-2.18 \times 10^{+2}$	$5.73 \times 10^{+2}$
b_{2j}	4.67×10^{-2}	1.77	-2.41	
a_{3j}	$1.92 \times 10^{+1}$	$-7.35 \times 10^{+2}$	$6.31 \times 10^{+2}$	$-1.73 \times 10^{+1}$
b_{3j}	1.06×10^{-1}	1.54	-2.57×10^{-1}	

TABLE XVIII. The coefficients of the least-squares fits to the parameters and coefficients of the three exponential fits for the directly computed dielectronic-recombination rate coefficients when the initial ion in one of the states $1s^22s2p^5{}^1P$ or 3P and the radiative transitions are $\Delta n \neq 0$: $\log_{10}(c_i) = \sum_{j=1}^4 a_{ij} z^{j-1}$, and $\xi_i = z^2 \sum_{j=1}^3 b_{ij} z^{1-j}$, where z is the effective charge of the initial ion.

j	1	2	3	4
State: $1s^22s2p^5{}^1P$				
a_{1j}	-8.39	-6.60	7.79	-2.14
b_{1j}	3.09×10^{-2}	5.44×10^{-1}	1.91	
a_{2j}	$-4.17 \times 10^{+1}$	$7.54 \times 10^{+1}$	$-5.76 \times 10^{+1}$	$1.50 \times 10^{+1}$
b_{2j}	1.09×10^{-1}	-2.48×10^{-1}	8.79	
a_{3j}	4.27	$-4.04 \times 10^{+1}$	$3.89 \times 10^{+1}$	$-1.15 \times 10^{+1}$
b_{3j}	1.54×10^{-1}	-3.69×10^{-1}	$1.17 \times 10^{+1}$	
State: $1s^22s2p^5{}^3P$				
a_{1j}	-3.89	$-1.68 \times 10^{+1}$	$1.55 \times 10^{+1}$	-4.09
b_{1j}	3.09×10^{-2}	5.45×10^{-1}	1.97	
a_{2j}	$-4.31 \times 10^{+1}$	$7.93 \times 10^{+1}$	$-6.08 \times 10^{+1}$	$1.59 \times 10^{+1}$
b_{2j}	1.00×10^{-1}	9.49×10^{-2}	6.31	
a_{3j}	$1.15 \times 10^{+1}$	$-5.64 \times 10^{+1}$	$5.07 \times 10^{+1}$	$-1.43 \times 10^{+1}$
b_{3j}	1.44×10^{-1}	4.54×10^{-2}	9.11	

ACKNOWLEDGMENTS

This work was supported by the Office of Fusion Energy of the Department of Energy and by Lawrence Liver-

more Laboratory. Most of the calculations were carried out on the computers of the National Magnetic Fusion Energy Computing Center.

- ¹L. J. Roszman, in *Physics of Electronic and Atomic Collisions*, edited by S. Datz (North-Holland, New York, 1982), p. 641.
- ²L. J. Roszman, Phys. Rev. A **35**, 2122 (1987).
- ³L. J. Roszman, Phys. Rev. A **20**, 673 (1979).
- ⁴L. J. Roszman, Phys. Rev. A **35**, 2138 (1987).
- ⁵D. E. Post, R. V. Jensen, C. B. Tarter, W. H. Grasberger, and W. A. Lokke, At. Data Nucl. Data Tables **20**, 397 (1977); R. A. Hulse, Bull. Am. Phys. Soc. **28**, 929 (1983); H. P. Summers and R. W. P. McWhirter, J. Phys. B **12**, 2387 (1979).
- ⁶M. D. Rosen, P. L. Hagelstein, D. L. Matthews, E. M. Campbell, A. U. Hazi, B. L. Whitten, B. MacGowan, R. E. Turner, and R. W. Lee, Phys. Rev. Lett. **54**, 106 (1985).
- ⁷L. J. Roszman, Fifth Topical Conference on Atomic Processes in High Temperature Plasmas, Monterey, California, 1985 (unpublished).
- ⁸A. Burgess, Astrophys. J. **141**, 1588 (1965).
- ⁹A. L. Merts, R. D. Cowan, and N. H. Magee, Jr., Los Alamos Scientific Laboratory Report No. LA-6220-MS, 1976 (unpublished).
- ¹⁰B. W. Shore, Astrophys. J. **158**, 1205 (1969).
- ¹¹D. R. Bates and A. Dalgarno, in *Atomic and Molecular Processes*, edited by D. R. Bates (Academic, New York, 1962), p. 245.
- ¹²R. D. Cowan, in *The Theory of Atomic Structure, and Spectra* (University of California Press, Berkeley, 1981), p. 197.
- ¹³M. E. Riley and D. G. Truhlar, J. Chem. Phys. **63**, 2182 (1975); **65**, 792 (1976).
- ¹⁴C. Frose, Can. J. Phys. **41**, 1895 (1963).
- ¹⁵E. C. Ridley, Proc. Cambridge Philos. Soc. **51**, 702 (1955).
- ¹⁶V. L. Jacobs, J. Davis, P. C. Kepple, and M. Blaha, Astrophys. J. **211**, 605 (1977).
- ¹⁷D. T. Woods, J. M. Shull, and C. L. Sarazin, Astrophys. J. **249**, 399 (1981).
- ¹⁸C. F. Fischer, Comput. Phys. Commun. **14**, 145 (1978).